Journal of NeuroEngineering and Rehabilitation

RESEARCH

Open Access

The effects of unilateral nostril breathing on brain functional network activity: a pilot study

David E. White[1,2*], Usman Ghani[2], Mangor Pedersen[3], Christian Thoma[4], Christi Essex[3], Daniel Shepherd[3], Georgina Burns[5], Toby S. Waterstone[2], K. L. T. Roos[2], Denise Taylor[6] and Imran K. Niazi[1,2,6]

Abstract

Background Unilateral nostril breathing (UNB) has a history linked to ancient yogic traditions where it is believed to affect both physical and mental states however the mechanism(s) by which this technique potentially influences brain electrical activity remains poorly explored.

Methods In this pilot study we investigated the influence of pressurised device-regulated UNB on brain functional network activity in healthy awake individuals to test its suitability for later use in hypothesis-driven clinical trials. Baseline bilateral EEG data were acquired, and then dominant/nondominant nostril UNB protocols were used to assess changes in brain network functional connectivity signal coherence, and phase lag index.

Results Changes in functional connectivity were detected only when comparing right to left UNB, with the following networks demonstrating changes: the Default Mode Network which included reduced alpha and increased beta wave activity; the Salience Network, which included increased gamma wave activity; the Auditory Network, which included increased gamma and delta wave activity; and the Left Brain Region, which included reduced delta wave activity.

Conclusions This study revealed that device-regulated pressurised left/right UNB changed brain FC in awake healthy individuals in several brain networks. Nasal cycle dominance was found to play no role in UNB influencing brain FC; rather, nasal morphology (left/right side) seems to be the controlling factor. Further investigations are needed to verify our results and apply them to clinical populations.

Keywords Unilateral nostril breathing, Electroencephalography, Functional network, Functional connectivity

*Correspondence:
David E. White
david.white@nzchiro.co.nz
[1]NZCC Research Centre, New Zealand College of Chiropractic, P. O. Box 113044, Newmarket, Auckland 1149, New Zealand
[2]Centre for Chiropractic Research, New Zealand College of Chiropractic, Auckland, New Zealand
[3]School of Psychology & Neuroscience, Auckland University of Technology, Auckland, New Zealand
[4]School of Interdisciplinary Studies, Auckland University of Technology, Auckland, New Zealand
[5]School of Physiotherapy, Auckland University of Technology, Auckland, New Zealand
[6]Rehabilitation Innovation Centre, Health & Rehabilitation Research Institute, Auckland University of Technology, Auckland, New Zealand

Introduction

There is growing evidence suggesting that respiration goes beyond gas exchange, with nasal breathing directly influencing cerebral rhythmic activity, sensory, affective, and cognitive functions [1–3]. During nasal breathing, respiration-linked olfactory bulb activity creates respiratory-modulated infraslow neural oscillations (ISNOs), ranging in frequency from 0.01 to 0.5 Hz [4, 5]. Both animal [6] and human studies [7] have shown that these nasal respiratory elicited ISNOs, which are strongly linked to the inspiratory phase of breathing [4], sweep across the brain and modulate higher neural oscillations in the delta (0.5–4 Hz), theta (4–8 Hz), alpha (8–13 Hz), beta (14–30 Hz), and gamma (30–50 Hz) ranges through cross-frequency phase amplitude coupling [8]. This amplitude modulated coupling facilitates information transfer across large-scale brain functional networks by improving coherence between communicating brain regions and suggests that the excitability of cortical networks, and hence human behavioural and task performance, is tightly linked to nasal breathing. Compared with mouth breathing, nasal breathing has been shown to enhance memory both during the awake-state [9] and after the sleep state [10]. During sleep, the interplay between nasal respiration-modulated ISNOs and sleep spindle complexes is thought to act as a pacemaker for sleep rhythms and memory consolidation [10]. With ISNOs being phase coupled to nasal breathing-elicited stimulation of airflow mechanoreceptors within the nose [11], it is not surprising that ISNO activity is significantly reduced or absent during mouth breathing, or when olfactory bulb neurons are pharmacologically suppressed [7, 12].

Nasal breathing has also been shown to modulate sensorimotor, cognitive, and emotional processes [7, 13], as well as the neural correlates of consciousness [14]. Given that nasal respiratory-coupled ISNOs are now considered critical for synchronizing information processing and network interactions across the brain during cognitive functioning [2, 13, 15], it is not surprising that oral breathing has been implicated in attention and learning impairment [16], poor sleep quality [17], and poor academic performance [18, 19].

It has been suggested that changes in brain functional connectivity (FC) across distinct brain networks might be a mechanism of neurological dysfunction and impaired cognitive performance [20, 21]. Abnormal FC has been reported in many neuropathological conditions including attention deficit hyperactivity disorder [22], posttraumatic stress disorder [23], schizophrenia [24], migraine [25], epilepsy [26], major depression [27], anxiety [28, 29], insomnia [30], and chronic pain [31].

Normal nasal airflow is cerebrally regulated, with the ultradian rhythm of periodic change in nasal airflow bias between each side of the nose termed 'the nasal cycle'. Here the side of the nose passing the greater airflow is termed 'dominant' and the other side 'nondominant' [32]. Multiple purpose(s) of the nasal cycle in regulating nasal air conditioning [33, 34] and brain activity [35] continue to be postulated and the role nasal airflow plays in influencing brain activity remains controversial. In particular, research on the influence of unilateral nostril breathing (UNB) on cognitive performance is inconsistent; some studies have reported this breathing technique influences cognitive performance [36–38] whereas others have reported that it has no effect [32, 39]. Despite this, a recent electroencephalographic (EEG) study of brain activity during UNB using cluster-based permutation tests revealed significant reductions in EEG spectral power across all bands during left-sided UNB, and all bands except delta for right-sided UNB vs. dual nostril breathing [40]. While this finding suggests that UNB could modify brain FC, and potentially mitigate many undesirable neuropathological conditions, the influence of UNB on brain activity remains poorly explored.

We are unaware of any other EEG studies in the current literature investigating how UNB affects neural network FC. Given the previously reported interplay between nasal breathing-elicited ISNOs and brain-state, and reports of the nasal cycle influencing cerebral activity, our research tests for any association between UNB and changes in FC across multiple brain networks and frequencies. This investigation used device-applied pressurised UNB to: (1) determine whether UNB changes brain network FC in healthy individuals; and (2) compare any changes in FC between left/right and dominant/nondominant UNB.

Materials and methods

Ethics approval and participant recruitment

This EEG study followed the Declaration of Helsinki and was approved by the AUT Ethics Committee (AUTEC, approval number 14/02). The participant exclusion criteria included recent upper-airway or sinus infection; a history of mental illness; presence of a respiratory condition or allergy; and current smokers or ex-smokers of less than five years. Thirty participants ($n = 19$ females, $n = 11$ males), ranging in age from 20 to 53 years, were recruited, with all participants providing written informed consent before study commencement.

Nasal breathing protocol

All participants received the same pressurised UNB protocol, delivered by a new type of nasal continuous positive airway pressure (n-CPAP) device, called the Rest-Activity-Cycler (RACer), developed at the Auckland University of Technology. This device delivers pressurised ambient air to the spontaneously nasal breathing participant,

with internasal airflow apportioned so that almost all the air passes exclusively through one nostril. Independent control of each nostril airflow is facilitated by a divider in the mask, enabling two separate pneumatic pathways to deliver different air flows to each side of the nose. For each participant, the side of the nose passing the dominant airflow was recorded prior to the nasal mask being fitted to determine their endogenous nasal cycle status at the commencement of data collection.

This study used the same sequence of regulated UNB during data collection described in more detail by Niazi, et al. [40]. To prevent confounding by face muscle artifacts, each participant wore goggles onto which the nasal breathing interface was mounted, and an initial 3-minute period was used to quantify baseline EEG activity corresponding to the participants' natural nasal breathing state. Here, the nasal mask was on but not pneumatically connected to the RACer system, and the participants breathed ambient air. After baseline data collection, the RACer device was activated to deliver a preset program of UNB control commencing with 90% of participants' tidal airflow passing through their dominant nostril at a maximal pressure of 8 cmH_2O. After 10-minutes of dominant-side UNB, the RACer system swaped sides of the nose to deliver 90% tidal airflow to the nondominant side of the nose for a further 10-minute period. Across participants, this served to randomize the order of the sides of the nose (left or right) initially experiencing UNB states.

Data collection

The Participants were instructed to pay attention to a silent film during EEG data acquisition and were advised that there would be a short test following the scan. This strategy removed the participants' focus from their breathing pattern and style to control for potential confounding variable that focus on, or mindfulness of, their breathing that might influence brain activity [41]. The use of long air hoses enabled the RACer device to be sited outside the soundproof and electrically shielded test environment.

EEG data acquisition

Cortical electrical activity was recorded at a sampling rate of 500 Hz via a 64-channel (10–20 system) EEG using NuAMPs (Compumedics Neuroscan, Inc., Charlotte, NC, USA). True electrode locations were co-registered to each participants' anatomy The ground electrode was placed next to Cz, and all impedances were kept below 5kΩ.

EEG data preprocessing

Preprocessing offline was performed via scripts developed in MATLAB version 2015b (The MathWorks, Inc., Natick, MA, USA.) and functions from toolboxes EEGLAB version 14.1.1 [42], ERPLAB version 6.1.4 [43], and FieldTrip version 20,180,912 [44]. This processing pipeline has been used previously by the research group [40] for resting-state EEG and evoked potentials [45, 46]. The removal of signals unrelated to brain activity, such as eye blinks, muscle activity and noise from channels and mains, and EEG data analysis, are described in detail Niazi, et al. [40]. After preprocessing, the EEG data were imported into Brainstorm in MATLAB R2021b for source reconstruction.

Data analysis

Sensor signals are complex mixtures from multiple brain regions, leading to overlapping signals and volume conduction at the sensor level [47], making it difficult to link EEG dynamics to specific anatomical regions. Therefore, this study looked at source reconstruction to link breathing-elicited changes to specific anatomical regions.

EEG source reconstruction

Using advanced mathematical models and algorithms, source reconstruction provides a comprehensive understanding of brain activity by identifying specific regions and networks involved in tasks or behaviors [48]. EEG source reconstruction was performed via Brainstorm in MATLAB R2022a (the detailed method is provided in supplementary material S1). Source reconstruction estimates the location and activity of underlying neural sources on the basis of measurements from multiple sensors or electrodes to provide a more comprehensive understanding of brain activity by identifying specific regions and networks involved in tasks (more details can also be found at Ref. [49]). Functional connectivity was then assessed by grouping high-resolution sources according to the Desikan Killiani atlas, which defines 68 regions of interest (ROIs) on the cortex surface, as shown in Fig. 1, enabling source estimation [50].

The time series data within each ROI were averaged to form a [ROIs x time] matrix. To prevent activity cancellation, accurately estimate brain activity, and understand brain region connectivity, the sign of dipoles with opposite directions was flipped before averaging. After the atlas was defined, we examined the FC between these ROIs to determine the effect of UNB on the brain.

After the source reconstruction, the data were divided into narrow-band signals via a 4th-order Butterworth filter before phase lag index (PLI) computation, which extracted specific frequency bands: delta (0.5–4 Hz), theta (4–8 Hz), alpha (7.5–12.5 Hz), beta (12.5–30 Hz), and gamma (30–40 Hz). PLI was computed between every reconstructed EEG source signal pair, resulting in PLI values ranging from zero (no connectivity) to one (maximum connectivity). PLI data were stored in a connectivity matrix of dimension ROI x ROI (68×68) with

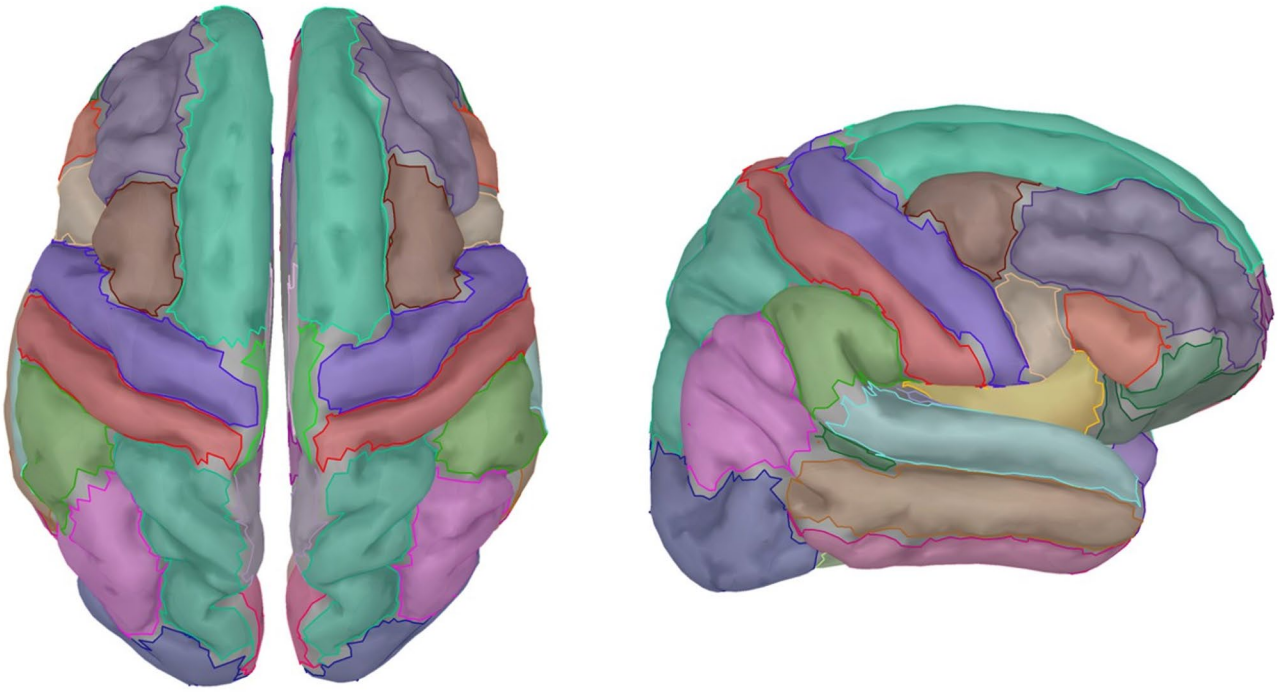

Fig. 1 Desikan Killiani atlas in brainstorm (MATLAB R2022a) defining 68 regions of interest on the cortex surface

zeros along the diagonal, giving a symmetric square matrix corresponding to the number of sources within the Desikan Killiani atlas. These matrices were generated for three conditions: (1) baseline, (2) dominant nostril breathing, and (3) nondominant nostril breathing within each frequency band. We then used nonparametric cluster-based permutations to find significant source pairs when we compared the abovementioned conditions.

Nonparametric cluster-based permutation

We implemented a nonparametric cluster-based permutation test to address the multiple comparison problem and maintain control over the familywise error rate [51]. Through a within-subject design, this analysis compared the computed PLI values across the adjacency matrices across three conditions (baseline vs. nondominant UNB, baseline vs. dominant UNB, and nondominant UNB vs. dominant UNB) within each defined network. The nonparametric cluster-based permutation analysis was executed via the FieldTrip toolbox (developed by the Donders Institute for Brain, Cognition, and Behaviour, Nijmegen, Netherlands). Cluster-level statistics were computed for each paired comparison (baseline vs. nondominant UNB, baseline vs. dominant UNB, and nondominant UNB vs. dominant UNB). The maximum cluster-level statistic was used as the critical t-value for identifying significant clusters. To establish a null distribution, we performed 5000 permutations by randomly reassigning the condition labels for each comparison. Cluster-level statistics were then recalculated for each permutation, representing the expected distribution of outcomes under the null hypothesis of no FC differences between conditions.

The p-value for each detected cluster was determined by calculating the proportion of permutations where the cluster-level statistic exceeded (either positively or negatively, depending on the direction) the observed cluster-level statistic. A significant positive cluster (+cluster) represented enhanced FC, whereas a significant negative cluster (-cluster) indicated reduced FC in one condition. This statistical approach enabled us to identify neural regions where FC exhibited significant changes between conditions, revealing how UNB modulates brain network dynamics. The findings were visualized on the cortical surface via EEGNET version 1 [52].

EEG functional connectivity analysis

All EEG participant data were analysed, and sixty seconds of clean resting-state EEG data used for the baseline that was compared to dominant/nondominant and left/right UNB states to determine effect changes for each breathing condition. Analysis was performed on the following brain networks: default mode network (DMN), dorsal attention network (DAN), salience network (SAN), auditory network (AUD), visual network (VIS), whole left-brain region (LBR) and whole right brain region (RBR). Three levels of comparison were performed for both the dominant/nondominant and left/right UNB states to determine whether changes in FC were elicited by UNB, as shown by Table 1. The purpose of this approach is to

Table 1 Three levels of comparison were undertaken for both the dominant/nondominant and left/right UNB States to determine the FC changes elicited by UNB

	Dominant/non-dominant UNB	Left/right UNB
Level 1 comparison	(D-B) Dominant UNB minus baseline	(L-B) Left UNB minus baseline
Level 2 comparison	(N-B) Non-dominant minus baseline	(R-B) Right UNB minus baseline
Level 3 comparison	(D-B)-(N-B)	(L-B)-(R-B)

identify whether nasal functional status (nasal cycle) or morphology (left/right), or both influence the results.

Functional connectivity was calculated to estimate the effects of lateralization, with the nonmirrored continuous channel data and dominance, and the data mirrored in the sagittal plane for participants with left nostril dominance. The use of both mirrored and nonmirrored data serves to check whether the patterns observed in the data are consistent across both representations. If both methods (mirrored and nonmirrored) yield the same outcome, then the findings are robust and not biased by the side being measured. Since the data analysis yielded the same outcome regardless of mirrored data, the Results section illustrates only the findings calculated from the nonmirrored data.

Spatio-spectral analysis was used to determine left and right UNB-elicited changes in brain FC across each of the neural networks under consideration via two types of analysis. Coherence in oscillations (amplitude and phase) between communicating regions was used to index the coupling of signalling between brain regions across different frequency bands [53] for the two different UNB states. The PLI was also used to measure asymmetry of brain signalling across different frequency bands [54] between each of the two different UNB states and baseline data to quantify the average phase difference distribution elicited by left and right UNB. PLI is less sensitive to volume conduction, and spurious zero-lag correlations between EEG signals [55]. Differences between UNB states were quantified via Cohen's d which calculates the standardized difference of means obtained during left and right UNB [56].

Data presentation

Brain regions of interest were visualized at the cortical level with FC between regions determined via EEGNET, an open-source tool for analysing and visualizing the EEG connectome. Regions of interest within specific functional networks are identified by coloured circles with changes in FC presented using coloured lines to indicate an increase or reduction.

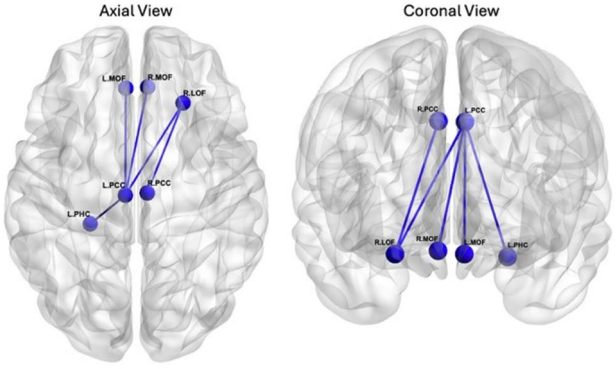

Fig. 2 Alpha functional connectivity between default mode network (DMN) brain regions. Visualization of the networks in the cortex revealed that FC occurred between regions of the brain during left and right UNB stimulation (L-B)-(R-B). Here, the blue shaded regions denote the DMN. The blue dots in the cortex visualization mark the brain regions that showed significant differences. The blue lines connecting the dots visualize the reduction in FC occurring between these brain regions during the two breathing states. Acronyms: R LOF (right lateral orbitofrontal), R PCC (right posterior cingulate cortex), L PCC (left posterior cingulate cortex), L MOF (left medial orbitofrontal), R MOF (right medial orbitofrontal), and L ParaH (left parahippocampal)

Results

At the beginning of testing, 12 participants were left nostril dominant, and 18 participants were right nostril dominant. No significant changes in FC were detected when dominant (dominant UNB minus baseline) and nondominant (nondominant UNB minus baseline) breathing states were compared. When comparing changes in left (left UNB minus baseline) to changes in right (right UNB minus baseline) nasal breathing states, represented as (L-B)-(R-B), frequency-specific decreases and increases in FC occurred in several brain regions comprising different functional brain networks. Only statistically significant changes in the EEG results are reported in detail within the following sections.

Alpha frequency connectivity

Only the default mode network (DMN) showed significant changes within the alpha band, as demonstrated by decreases in alpha frequency connectivity across several brain regions between left to right UNB states. Figure 2 presents the DMN regions, shown in blue circles, where FC was significantly different (t (DF) = -12.247, $p = 0.005$), along with a significant reduction in the brain signalling PLI, shown by the dark blue lines linking the DMN brain regions.

Significant changes in FC between brain regions and effect size were also detected in the alpha frequency band when comparing left to right nostril stimulation to baseline (*re*: Table 2). While no significant change in coherence was found, a comparison of significant changes in the PLI during right and left UNB is given in Table 2.

Table 2 Changes in alpha wave functional connectivity between default mode network brain regions

	Cluster ($p = 0.0080$)	Effect size (Cohen's d)	PLI during Right UNB	PLI during Left UNB
Alpha - DMN Left vs. Right UNB (L-B)-(R-B)	R LOF – R PCC	– 0.1239	0.0073 (+/– 0.0384)	0.0413 (+/– 0.0906)
	R LOF – L PCC	– 0.1257	0.0069 (+/– 0.0366)	0.0406 (+/– 0.0892)
	L MOF – L PCC	– 0.1884	0.0069 (+/– 0.0367)	0.0607 (+/– 0.1094)
	R MOF – L PCC	– 0.1451	0.0093 (+/– 0.0494)	0.0506 (+/– 0.0995)
	L PHC – L PCC	– 0.1259	0.0182 (+/– 0.0669)	0.0563 (+/– 0.1147)
	L PHC – R PCC	– 0.1366	0.0185 (+/– 0.0686)	0.0612 (+/– 0.1106)

The results for right UNB stimulation, left UNB stimulation and effect size (Cohen's d) for the significant cluster within the alpha band

See Fig. 2 for acronyms

Table 3 Changes in beta wave functional connectivity between default mode network brain regions

	Cluster ($p = 0.0188$)	Effect size (Cohen's d)	PLI during Right UNB	PLI during Left UNB
Beta - DMN Left vs. Right UNB (L-B)-(R-B)	L LOF – L PCC	0.1418	0.0291 (+/– 0.0572)	0.0084 (+/– 0.0312)
	R LOF – L PCC	0.1510	0.0324 (+/– 0.0578)	0.0097 (+/– 0.0356)
	R LOF – R PCC	0.1538	0.0403 (+/– 0.0599)	0.0148 (+/– 0.0438)
	L MOF – R PCC	0.1541	0.0329 (+/– 0.0584)	0.0092 (+/– 0.0339)
	L MOF – L PCC	0.1353	0.0395 (+/– 0.0592)	0.0188 (+/– 0.0472)
	L MOF – R PCH	–	0.0172 (+/– 0.0432)	0

The results for right stimulation, left stimulation and effect size (Cohen's d) for the significant cluster within the beta band

See Fig. 3 for acronyms

Beta frequency connectivity

Only the DMN also showed significant connectivity changes in the beta band. Increased beta FC occurred within the DMN when comparing left to right UNB stimulation across several brain regions, which formed one cluster in the nonparametric cluster-based permutation test. Figure 3 presents the DMN brain regions, shown by red circles, whose FC was significantly increased ($t(DF) = 12.652$, $p = 0.005$), and with a significant increase in the PLI, presented as red lines.

Significant increases in FC between brain regions occurred between left and right UNB stimulation in the beta frequency band. The effect sizes for these changes across brain regions are presented in Table 3. While no significant change in signal coherence was found, comparisons of significant changes in the PLI during right and left UNB are also provided.

Gamma frequency connectivity

The salience network (SAN) and the auditory network (AUD) both showed significant changes within the

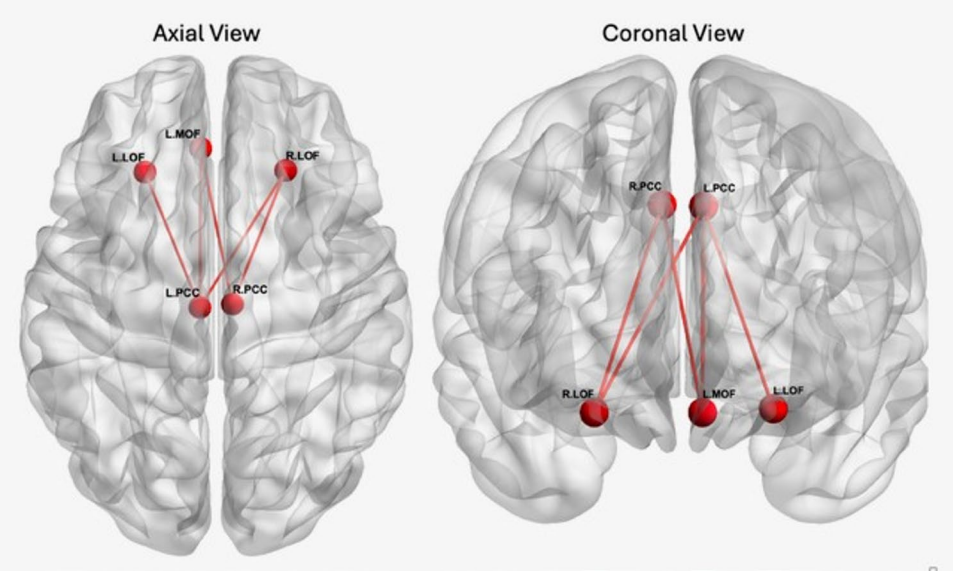

Fig. 3 Changes in beta functional connectivity between default mode network (DMN) brain regions. Visualization of the networks in the cortex showing FC between brain regions between right and left UNB stimulation (L-B)-(R-B). Here, the red shaded circular regions denote DMN regions that showed significant differences. The red lines connecting these circles visualize the increase in FC occurring between these brain regions between the two breathing states. Acronyms: L PCC (left posterior cingulate cortex), R PCC (right posterior cingulate cortex), L MOF (left medial orbitofrontal), L LOF (left lateral orbitofrontal), R LOF (right lateral orbitofrontal), and L ParaH (left parahippocampal)

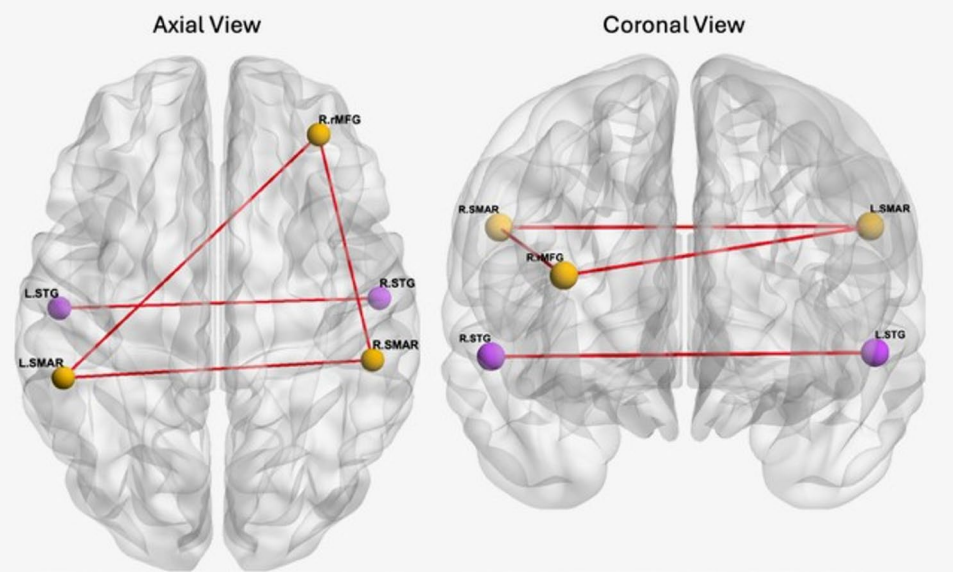

Fig. 4 Changes in gamma functional connectivity between salience network (SAN) and audible network (AUD) brain regions. Visualization of the networks in the cortex shows the differences in FC occurring between these regions within the brain between right and left UNB stimulation (L-B)-(R-B). Here, the orange and purple shaded circles denote regions within the SAN and AUD respectively. Both of these networks experienced increases in gamma frequency FC, shown by orange lines, between left and right UNB stimulation between the two breathing states. Acronyms: R rMFG (right rostral middle frontal), L SMAR (left supramarginal), and R SMAR (right supramarginal)

Table 4 Changes in gamma wave functional connectivity between salience and audible network brain regions

	1 cluster ($p = 0.0324$)	Effect size (Cohen's d)	PLI during Right UNB	PLI during Left UNB
Gamma - SAN Left vs. Right UNB (L-B)-(R-B)	R rMFG – L SMAR	0.1403	0.0294 (+/− 0.0575)	0.0101 (+/− 0.0376)
	R rMFG – R SMAR	0.2042	0.0483 (+/− 0.0664)	0.0208 (+/− 0.0525)
	L SMAR – R SMAR	0.3013	0.0548 (+/v 0.0696)	0.0146 (+/− 0.0429)
Gamma -AUD Left vs. Right UNB (L-B)-(R-B)	1 cluster ($p = 0.0004$)	-	-	-
	L STG – R STG	0.4882	0.0991 (+/− 0.2169)	0.0176 (+/− 0.0933)

The results of right UNB, left UNB, and effect size (Cohen's d) for the significant cluster within the gamma band

See Fig. 4 for acronyms

gamma band where FC increased between left and right UNB stimulation. For the SAN regions, as shown by the orange circles in Fig. 4, one cluster's FC significantly increased, as shown by the orange lines, ($t(DF) = 6.3866$, $p = 0.005$). For AUD regions, shown by the purple circles in Fig. 4, FC in the gamma frequency band also increased, as shown by the orange lines, between left and right UNB stimulation across several brain regions, forming a single cluster ($t(DF) = 2.1754$, $p = 0.005$).

Table 4 presents the FC values for the SAN and AUD brain regions, separately highlighting significant changes observed between left and right UNB stimulation in the gamma frequency band, as well as the effect size of these changes between brain regions. While no significant change in signal coherence was identified, a comparison of the significant changes in the PLI during right and left UNB is also provided.

Delta frequency connectivity

The auditory network (AUD) and left-brain region (LBR) showed significant changes within the delta band. FC in the delta frequency increased from right to left UNB stimulation in several AUD and LBR regions, forming a single cluster in the nonparametric cluster-based permutation test ($t(DF) = 1.9040$, $p = 0.005$) and ($t = 9.2808$, $p = 0.005$) respectively. The AUD brain regions with significantly different FC are highlighted in purple in Fig. 5, and experienced increased coherency, indicated by red lines. LBR regions, indicated by green circles, experienced reduced delta frequency coherency, indicated by blue lines.

Table 5 presents the FC values for the AUD and LBR separately, showing significant changes in the effect size of these changes between left and right UNB stimulation in the alpha frequency band. While no significant change in the PLI was observed, a comparison of the significant changes in signal coherence from left to right UNB was also included.

Theta frequency connectivity

No significant changes in FC were found in any brain region in the theta band.

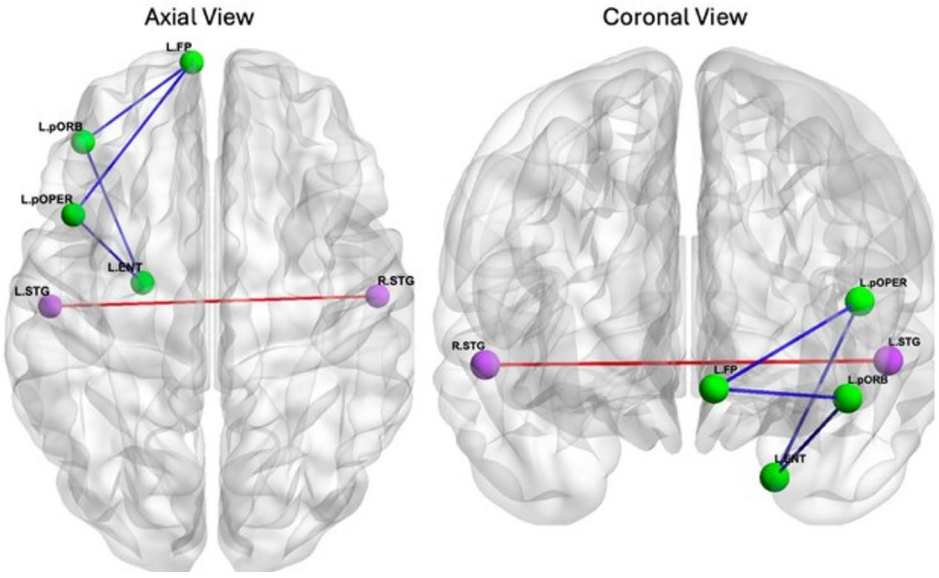

Fig. 5 Changes in delta functional connectivity between auditory network (AUD) and left brain region (LBR). Visualization of the networks in the cortex shows the differences in FC occurring between the regions within the brain between right and left UNB stimulation (L-B)-(R-B). Here, the purple circles represent the AUD brain regions with significantly different FC that experienced increased coherence, as indicated by the red line. LBR regions, indicated by green circles, experienced reduced delta frequency coherency, indicated by blue lines. .Acronyms: R STG (right superior temporal), L STG (left superior temporal), L ENT (left entorhinal), L FP (left frontal pole), L pORB (left parsorbitalis), and L pOPER (left parsopercularis)

Table 5 Changes in delta wave functional connectivity between left brain region and audible network brain regions

	1 cluster ($p = 0.0248$)	Effect size (Cohen's d)	Coherence during Right UNB	Coherence during Left UNB
Delta - LBR Left vs. Right UNB (L-B)-(*R*-B)	L pOPER – L ENT	– 0.1032	0.1786 (+/– 0.3166)	0.2939 (+/– 0.3284)
	L pOPER – L FP	– 0.1245	0.0189 (+/– 0.1002)	0.1572 (+/– 0.2798)
	L pORB - L ENT	– 0.0768	0.0869 (+/– 0.2173)	0.1677 (+/– 0.2714)
	L pORB – L FP	– 0.1244	0.0985 (+/– 0.2492)	0.2323 (+/– 0.3220)
Delta - AUD Left vs. Right UNB (L-B)-(R-B)	L STG – R STG	0.3326	0.1071 (+/– 0.2346)	0.0414 (+/– 0.1523)

The results of right UNB stimulation, left UNB stimulation, and effect size (Cohen's d) for the significant cluster within the delta band

See Fig. 5 for acronyms

Discussion

Frequency and network specific changes

Our study revealed significant changes in FC across different brain frequencies when comparing right to left UNB with baseline data subtraction; however, we observed no significant change when comparing left or right UNB to the baseline state. This latter finding suggests that the participants' natural breathing state did not influence the results.

No significant changes in FC were found when dominant/nondominant UNB was compared with baseline data subtraction to the right to left UNB with baseline data subtraction, suggesting that nasal morphology (left/right) and not nasal cycle status regulates UNB FC results. Additionally, this finding demonstrated that the silent film had no influence on the results given that participants demonstrated different nasal cycle statuses (12 left dominant and 18 right dominant) at the commencement of synchronized data collection and film observation.

Changes in DMN FC coherence in both alpha and beta frequencies have previously been reported in sufferers of, anxiety [28], chronic pain [31], and attention-hyperactivity disorders [22]. Our findings of reduced alpha and increased beta FC imply the potential for left UNB to beneficially modify attentional and self-sensory-motor processing functions [57] of these individuals. On the other hand, right UNB could benefit patients with Schizophrenia given that this breathing strategy results in reduced DMN delta and increased alpha brain activity [24]. This latter suggestion is supported by a previous study reporting the use of right UNB to successfully treat hallucinations in an adult schizophrenic patient [58].

The SAN is involved in detecting and filtering salient stimuli, task switching, and recruiting other divergent functional networks by contributing to a variety of complex functions that influence our actions, emotions, and reactions [59]. While synchronization of gamma waves within the SAN is crucial for multisensory integration and information transmission [60], elevated gamma activity within this network is associated with insomnia

[30], depression [27], and PTSD [61]. Our finding that the right UNB suppressed gamma FC within this network suggests that this breathing strategy could be used to mediate these neuropathological states.

Despite quiet study conditions, increased FC activity was found to occur within the AN network in the gamma and delta frequencies, suggesting that left UNB could upregulate auditory perceptions [62].

The LBR controls many functions, including speech implementation, analytical tasks and sleep, with delta waves associated with deep sleep states [63]. During sleep, particularly non-REM (NREM) slow-wave sleep (stages 3–4 NREM), the left hemisphere in particular exhibits high delta activity [64]. During normal sleep, nasal cycle airflow bias presents as a regular exchange between left and right-sided nasal airflow dominance during NREM and REM sleep, respectively [65]. Our findings that brain delta activity increases within the AN but decreases within the left brain during left and right UNB suggests that nasal airflow regulation could be associated with the dynamics of nasal air flow/sleep-stage interplay; however, this topic remains poorly understood and further investigation is needed.

The purpose of this pilot study was to investigate whether device-regulated pressurised UNB could influence brain FC in healthy individuals. Our findings suggest that this breathing strategy changes FC in some brain networks but only with left/right UNB techniques rather than with reference to dominant/nondominant nasal cycle status. Our results suggest that left/right UNB can modulate abnormal brain FC to potentially treat various neuropathological states however, this topic remains poorly understood and further study is needed.

Study limitations

This pilot study sought to identify whether specific changes in FC within specific brain functional networks could be elicited by UNB. While our results demonstrate the potential of UNB as a breathing neurotherapy, there is much more research required into this topic. For example, it is not known if the healthy awake participants in this investigation demonstrate the same FC responses to UNB stimuli compared to a cohort experiencing one of the neuropathological states described earlier. We also acknowledge that this exploratory study does not investigate the mechanisms by which UNB affects brain FC or examine any specific FC neuropathological state in detail. Despite these limitations, our findings support the need for future research into the potential of using UNB as a breathing neurotherapy.

Conclusions

Device-regulated pressurised left/right UNB changes brain FC in awake healthy individuals at some frequencies in some brain networks. Nasal cycle dominance plays no role in UNB influencing brain FC, rather, nasal morphology (left/right side) seems to be the controlling factor. Further investigations are needed to verify our results and apply them to clinical populations.

Supplementary Information

The online version contains supplementary material available at https://doi.org/10.1186/s12984-025-01782-x.

Supplementary Material 1.

Acknowledgements

Not applicable.

Author contributions

DEW proposed and oversaw the study, and was the largest contributor to the manuscript. UG assisted in the EEG analysis and contributed to the manuscript preparation and editing. GB undertook data collection and assisted in data analysis. MP, CT, and CE assisted in the interpretation of results and contributed to manuscript preparation and editing. DS designed the study protocol, supervised the study and data collection, and contributed to manuscript preparation and editing. TW performed the data and statistical analysis, produced all figures and tables, and contributed to manuscript preparation and editing. KLTR advised the group and contributed to manuscript preparation and editing. DT assisted in the interpretation of results and contributed to manuscript preparation and editing. IKN oversaw data collection, data analysis and interpretation of results, and contributed to manuscript preparation and editing. All authors have reviewed the manuscript.

Funding

This research was self-funded by the research team.

Data availability.

While participant data cannot be shared openly to protect an individual's privacy, anonymized data are available upon request to the corresponding author (DEW).

Data availability

No datasets were generated or analysed during the current study.

Declarations

Ethics approval and consent to participate

This EEG study followed the Declaration of Helsinki and was approved by the Auckland University of Technology Ethics Committee (AUTEC, approval number 14/02). All participants provided written informed consent prior to their participation.

Consent for publication

DEW is listed inventor of the RACer pressurized breathing technology. All other authors declare no competing interest.

Competing interests

DEW is listed inventor of the RACer pressurized breathing technology. All other authors declare no competing interest.

Received: 15 June 2024 / Accepted: 15 October 2025
Published online: 15 December 2025

References

1. Allen M, Varga S, Heck DH. Respiratory rhythms of the predictive Mind. Psychol Rev. 2022. https://doi.org/10.1037/rev0000391.
2. Heck DH, et al. Cortical rhythms are modulated by respiration. BioRxiv. 2016;049007. https://doi.org/10.1101/049007.
3. Brændholt M, et al. Breathing in waves: Understanding respiratory-brain coupling as a gradient of predictive oscillations. Neurosci Biobehav Rev. 2023;152:105262. https://doi.org/10.1016/j.neubiorev.2023.105262.
4. Monto S, Palva S, Voipio J, Palva JM. Very slow EEG fluctuations predict the dynamics of stimulus detection and Oscillation amplitudes in humans. J Neuroscience: Official J Soc Neurosci. 2008;28:8268–72. https://doi.org/10.1523/JNEUROSCI.1910-08.2008.
5. Prokhorov MD, et al. Changes in the power and coupling of Infra-Slow oscillations in the signals of EEG leads during Stress-Inducing cognitive tasks. Appl Sci. 2023;13:8390.
6. Liu Y, McAfee SS, Heck DH. Hippocampal sharp-wave ripples in awake mice are entrained by respiration. Sci Rep. 2017;7:8950. https://doi.org/10.1038/s41598-017-09511-8.
7. Zelano C, et al. Nasal respiration entrains human limbic oscillations and modulates cognitive function. J Neurosci. 2016;36:12448–67. https://doi.org/10.1523/jneurosci.2586-16.2016.
8. Canolty RT, Knight RT. The functional role of cross-frequency coupling. Trends Cogn Sci. 2010;14:506–15. https://doi.org/10.1016/j.tics.2010.09.001. https://doi.org/https://doi.org/.
9. Arshamian A, Iravani B, Majid A, N Lundström J. Respiration modulates olfactory memory consolidation in humans. J Neurosci. 2018;3360–3317. https://doi.org/10.1523/JNEUROSCI.3360-17.2018.
10. Schreiner T, Petzka M, Staudigl T, Staresina BP. Respiration shapes sleep-oscillations and memory reactivation in humans. *bioRxiv*, 2023.2003.2016.532910 (2023). https://doi.org/10.1101/2023.03.16.532910
11. Väyrynen T, et al. Infra-slow fluctuations in cortical potentials and respiration drive fast cortical EEG rhythms in sleeping and waking States. Clin Neurophysiol. 2023;156:207–19. https://doi.org/10.1016/j.clinph.2023.10.013.
12. González J, et al. Breathing modulates gamma synchronization across species. Pflugers Arch. 2023;475:49–63. https://doi.org/10.1007/s00424-022-02753-0.
13. Heck DH, et al. Breathing as a fundamental rhythm of brain function. Front Neural Circuits. 2017;10. https://doi.org/10.3389/fncir.2016.00115.
14. Piarulli A, et al. Ultra-slow mechanical stimulation of olfactory epithelium modulates consciousness by slowing cerebral rhythms in humans. Sci Rep. 2018;8:6581. https://doi.org/10.1038/s41598-018-24924-9.
15. Tort ABL, Brankačk J, Draguhn A. Respiration-Entrained brain rhythms are global but often overlooked. Trends Neurosci. 2018;41:186–97. https://doi.org/10.1016/j.tins.2018.01.007.
16. Ghazvineh S, et al. Rhythmic air-puff into nasal cavity modulates activity across multiple brain areas: A non-invasive brain stimulation method to reduce ventilator-induced memory impairment. Respir Physiol Neurobiol. 2021;287:103627. https://doi.org/10.1016/j.resp.2021.103627.
17. Young T, Finn L, Kim H. Nasal obstruction as a risk factor for sleep-disordered breathing. J Allergy Clin Immunol. 1997;99:S757–62. https://doi.org/10.1016/S0091-6749(97)70124-6. https://doi.org/http:.
18. Jung J-Y, Kang C-K. Investigation on the effect of oral breathing on cognitive activity using functional brain imaging. Healthc (Basel). 2021;9:645. https://doi.org/10.3390/healthcare9060645.
19. Lee K-J, Park C-A, Lee Y-B, Kim H-K, Kang. C.-K. EEG signals during mouth breathing in a working memory task. Int J Neurosci. 2020;130:425–34. https://doi.org/10.1080/00207454.2019.1667787.
20. Brandl F, et al. Common and specific large-scale brain changes in major depressive disorder, anxiety disorders, and chronic pain: a transdiagnostic multimodal meta-analysis of structural and functional MRI studies. Neuropsychopharmacology. 2022. https://doi.org/10.1038/s41386-022-01271-y.
21. Cassidy JM, Mark JI, Cramer SC. Functional connectivity drives stroke recovery: shifting the paradigm from correlation to causation. Brain. 2021;145:1211–28. https://doi.org/10.1093/brain/awab469.
22. Cannon R, Cynthia K, Adam Hand, Garner CL. Pilot data assessing the functional integrity of the default network in adult ADHD with fMRI and sLORETA. J Neurotherapy. 2012;16:246–63. https://doi.org/10.1080/10874208.2012.730408.
23. Lee S-H, Yoon S, Kim J-I, Jin S-H, Chung CK. Functional connectivity of resting state EEG and symptom severity in patients with post-traumatic stress disorder. Prog Neuropsychopharmacol Biol Psychiatry. 2014;51:51–7. https://doi.org/10.1016/j.pnpbp.2014.01.008.
24. Baenninger A, et al. Abnormal coupling between default mode network and delta and beta band brain electric activity in psychotic patients. Brain Connect. 2017;7:34–44. https://doi.org/10.1089/brain.2016.0456.
25. Hsiao F-J, et al. Characteristic oscillatory brain networks for predicting patients with chronic migraine. J Headache Pain. 2023;24:139. https://doi.org/10.1186/s10194-023-01677-z.
26. Wang Y, et al. Altered neuromagnetic activity in default mode network in childhood absence epilepsy. Front Neurosci. 2023;17. https://doi.org/10.3389/fnins.2023.1133064.
27. Dai Z, et al. Disrupted fronto-parietal network and default-mode network gamma interactions distinguishing suicidal ideation and suicide attempt in depression. Prog Neuropsychopharmacol Biol Psychiatry. 2022;113:110475. https://doi.org/10.1016/j.pnpbp.2021.110475.
28. Imperatori C, et al. Default mode network alterations in individuals with high-trait-anxiety: an EEG functional connectivity study. J Affect Disord. 2019;246:611–8. https://doi.org/10.1016/j.jad.2018.12.071.
29. Sylvester CM, et al. Functional network dysfunction in anxiety and anxiety disorders. Trends Neurosci. 2012;35:527–35. https://doi.org/10.1016/j.tins.2012.04.012.
30. Chen MC, Chang C, Glover GH, Gotlib IH. Increased Insula coactivation with salience networks in insomnia. Biol Psychol. 2014;97:1–8. https://doi.org/10.1016/j.biopsycho.2013.12.016.
31. Zinn ML, Zinn MA, Jason LA. Intrinsic functional hypoconnectivity in core neurocognitive networks suggests central nervous system pathology in patients with myalgic encephalomyelitis: A pilot study. Appl Psychophysiol Biofeedback. 2016;41:283–300. https://doi.org/10.1007/s10484-016-9331-3.
32. Samantaray S, Telles S. Nostril dominance at rest associated with performance of a left hemisphere-specific cancellation task. Int J Yoga. 2008;1:56–9. https://doi.org/10.4103/0973-6131.43542.
33. Pendolino A, Lund V, Nardello E, Ottaviano G. The nasal cycle: a comprehensive review. Rhinology Online. 2018;1:67–76.
34. White DE, Bartley J, Nates R. Model demonstrates functional purpose of the nasal cycle. Biomed Eng Online. 2015;14:11. https://doi.org/10.1186/s12938-015-0034-4.
35. Price A, Eccles R. Nasal airflow and brain activity: is there a link? J Laryngology Otology. 2016;1–6. https://doi.org/10.1017/S0022215116008537.
36. Block RA, Arnott DP, Quigley B, Lynch WC. Unilateral nostril breathing influences lateralized cognitive performance. Brain Cogn. 1989;9:181–90. https://doi.org/10.1016/0278-2626(89)90028-6.
37. Jella SA, Shannahoff-khalsa DS. The effects of unilateral forced nostril breathing on cognitive performance. Int J Neurosci. 1993;73:61–8. https://doi.org/10.3109/00207459308987211.
38. Shannahoff-khalsa DS, Boyle MR, Buebel ME. The effects of unilateral forced nostril breathing on cognition. Int J Neurosci. 1991;57:239–49. https://doi.org/10.3109/00207459109150697.
39. Santhanam Kumar SS, Kamath A, Poojary S. Effect of unilateral left nostril breathing (Chandra Anga Pranayama) on cognitive function in healthy Yoga-Naïve individuals: A Randomized, Controlled, pilot study. Complement Med Res. 2020;27:319–27. https://doi.org/10.1159/000506972.
40. Niazi IK, et al. EEG signatures change during unilateral yogi nasal breathing. Sci Rep. 2022;12:520. https://doi.org/10.1038/s41598-021-04461-8.
41. Moore A, Gruber T, Derose J, Malinowski P. Regular, brief mindfulness meditation practice improves electrophysiological markers of attentional control. Front Hum Neurosci. 2012;6:18. https://doi.org/10.3389/fnhum.2012.00018.
42. Delorme A, Makeig S. EEGLAB: an open source toolbox for analysis of single-trial EEG dynamics including independent component analysis. J Neurosci Methods. 2004;134:9–21. https://doi.org/10.1016/j.jneumeth.2003.10.009.
43. Lopez-Calderon J, Luck SJ. ERPLAB: an open-source toolbox for the analysis of event-related potentials. Front Hum Neurosci. 2014;8:213. https://doi.org/10.3389/fnhum.2014.00213.
44. Oostenveld R, Fries P, Maris E, Schoffelen JM. FieldTrip: open source software for advanced analysis of MEG, EEG, and invasive electrophysiological data. Comput Intell Neurosci. 2011;2011(156869). https://doi.org/10.1155/2011/156869.
45. Navid MS, et al. Investigating the effects of chiropractic spinal manipulation on EEG in stroke patients. Brain Sci. 2020;10. https://doi.org/10.3390/brainsci10050253.
46. Navid MS, et al. The effects of chiropractic spinal manipulation on central processing of tonic pain - a pilot study using standardized low-resolution brain electromagnetic tomography (sLORETA). Sci Rep. 2019;9:6925. https://doi.org/10.1038/s41598-019-42984-3.

47. Rutkove SB. In: Blum AS, Seward B, Rutkove, editors. The clinical neurophysiology primer. Humana; 2007. pp. 43–53.
48. Friston K. Dynamic causal modeling and Granger causality comments on: the identification of interacting networks in the brain using fMRI: model selection, causality and Deconvolution. NeuroImage. 2011;58:303–5. https://doi.org/10.1016/j.neuroimage.2009.09.031. author reply 310 – 301.
49. Ghani U, et al. The influence of multiple cognitive workload levels of an exergame on dorsal attention network connectivity at the source level. Physiol Behav. 2024;284:114628.https://doi.org/10.1016/j.physbeh.2024.114628.
50. Kabbara A, El Falou W, Khalil M, Wendling F, Hassan M. The dynamic functional core network of the human brain at rest. Sci Rep. 2017;7:2936. https://doi.org/10.1038/s41598-017-03420-6.
51. Maris E, Oostenveld R. Nonparametric statistical testing of EEG- and MEG-data. J Neurosci Methods. 2007;164:177–90. https://doi.org/10.1016/j.jneumeth.2007.03.024. https://doi.org/https://doi.org/.
52. Hassan M, Shamas M, Khalil M, Falou E, W., Wendling FEEGNET. An open source tool for analyzing and visualizing M/EEG connectome. PLoS ONE. 2015;10:e0138297. https://doi.org/10.1371/journal.pone.0138297.
53. Srinivasan R, Winter WR, Ding J, Nunez PL. EEG and MEG coherence: measures of functional connectivity at distinct Spatial scales of neocortical dynamics. J Neurosci Methods. 2007;166:41–52. https://doi.org/10.1016/j.jneumeth.2007.06.026.
54. Stam CJ, Nolte G, Daffertshofer A. Phase lag index: assessment of functional connectivity from multi channel EEG and MEG with diminished bias from common sources. Hum Brain Mapp. 2007;28:1178–93. https://doi.org/10.1002/hbm.20346.
55. Peraza LR, Asghar AU, Green G, Halliday DM. Volume conduction effects in brain network inference from electroencephalographic recordings using phase lag index. J Neurosci Methods. 2012;207:189–99. https://doi.org/10.1016/j.jneumeth.2012.04.007.
56. Meyer M, Lamers D, Kayhan E, Hunnius S, Oostenveld R. Enhancing reproducibility in developmental EEG research: BIDS, cluster-based permutation tests, and effect sizes. Dev Cogn Neurosci. 2021;52:101036. https://doi.org/10.1016/j.dcn.2021.101036.
57. Fingelkurts AA, Fingelkurts AA, Bagnato S, Boccagni C, Galardi G. DMN operational synchrony relates to Self-Consciousness: evidence from patients in vegetative and minimally conscious States. Open Neuroimag J. 2012;6:55–68. https://doi.org/10.2174/1874440001206010055.
58. Shannahoff-Khalsa D, Golshan S. Nasal cycle dominance and hallucinations in an adult schizophrenic female. Psychiatry Res. 2015;226:289–94. https://doi.org/10.1016/j.psychres.2014.12.065.
59. Schimmelpfennig J, Topczewski J, Zajkowski W, Jankowiak-Siuda K. The role of the salience network in cognitive and affective deficits. Front Hum Neurosci. 2023;17. https://doi.org/10.3389/fnhum.2023.1133367.
60. Misselhorn J, Schwab BC, Schneider TR, Engel AK. Synchronization of Sensory Gamma Oscillations Promotes Multisensory Communication. *eNeuro* 6 (2019). https://doi.org/10.1523/eneuro.0101-19.2019
61. Abdallah CG, et al. Salience network disruption in U.S. Army soldiers with posttraumatic stress disorder. Chronic Stress (Thousand Oaks). 2019;3. https://doi.org/10.1177/2470547019850467.
62. Ying J, Zhou D, Lin K, Gao X. Network analysis of functional brain connectivity driven by Gamma-Band auditory Steady-State response in auditory hallucinations. J Med Biol Eng. 2015;35:45–51. https://doi.org/10.1007/s40846-015-0004-0.
63. Bernardi G, et al. Regional delta waves in human rapid eye movement sleep. J Neurosci. 2019;39:2686–97. https://doi.org/10.1523/jneurosci.2298-18.2019.
64. Dang-Vu TT et al. Spontaneous neural activity during human slow wave sleep. *Proceedings of the National Academy of Sciences* 105, 15160–15165 (2008). https://doi.org/10.1073/pnas.0801819105
65. Kimura A, et al. Phase of nasal cycle during sleep tends to be associated with sleep stage. Laryngoscope. 2013;n/a(n/a). https://doi.org/10.1002/lary.23986.

Publisher's note